Intelligent Real-time Land-movement Monitoring System (IRLMS)

THE HONG KONG UNIVERSITY OF SCIENCE AND TECHNOLOGY | The Division of Integrative Systems and Design (ISD)

HKUST ISD 2021-2022 Final Year Project Group ALI Final Report
Advisor:
Prof. Chi Ying TSUI (HKUST ISD)
Prof. Kai TANG (HKUST MAE)
Authors sorted alphabetically

Mark Anthony FUNG
The Division of ISD
The HKUST
Clear Water Bay, Hong Kong
mafung@connect.ust.hk

Qiucan HUANG
The Division of ISD
The HKUST
Clear Water Bay, Hong Kong
qhuangag@connect.ust.hk

Sai Kit TANG
The Division of ISD
The HKUST
Clear Water Bay, Hong Kong
sktangad@connect.ust.hk

Yifei LIN
The Division of ISD
The HKUST
Clear Water Bay, Hong Kong
ylinbz@connect.ust.hk

Yuchen LIANG
The Division of ISD
The HKUST
Clear Water Bay, Hong Kong
yliangbk@connect.ust.hk

***Abstract*—This document is an group report of HKUST ISD 2021-2022 final year project. The report found that the existing land-movement monitoring solution in the construction industry is frequently used yet inconvenient. So an Intelligent Real-Time Land-movement Monitoring System (IRLMS) including two methods, Smart Inclinometer (SInc) method and Meter In a Tube (MIT) is proposed to make the ground monitoring process real-time and affordable while providing a better user experience compared to existing solutions. Functional prototypes are built and tested. Though improvement still can be made, the prototypes worked as expected. Both method performed equally as the current traditional inclinometer using method and better in data refreshing rate, data manipulation and user interaction. Both methods also leaves potential for building construction IoT system in the future.**

***Index Terms*—construction robotics, inclinometer, strain gauge, land-movement monitoring**

I. Introduction

This project is 2021-2022 HKUST ISD final year project which, like other ISD projects, contains the following procedures:

- Topic selection: The team need to scope a topic to focus on to begin their project. This depends on the target users or companies.
- Problem defining: The team need to perform observation, site visit, interviews and investigation to define a problem that they want to solve. After conversations and desk research, this project team focus on land-movement monitoring.
- Literature review: After defining the problem, the team looks for existing solution that solve the similar problem.
- Idea generation: Several ideas will be generated by brainstorm. The team will select one or several ideas and try to make then into practice.
- Technology research: The team will then research for technology to realize the idea.
- Prototyping: A functioning prototype will be built to justify the idea.
- Testing: The team will use the prototype to test the functionality and performance compared to current solutions.

Therefore, this document will go through all the process stated above.

This project is done with Hong Kong construction company Paul Y. Engineering. The team focus on land-movement monitoring and vision a system to make land-monitoring more intelligent and user-friendly. The team go through the problem defining, literature review process and generate two ideas (methods). In order to experiment on all possibilities, the team chose to implement both ideas. Two functional prototypes are built and testing are done to evaluate the ideas. At last conclusion and summary are made.

II. Working principle of a inclinometer

A inclinometer is defined as an instrument for measuring the slope of a surface with respect to the vertical. [1] It measures data using an IMU inside and communicate with outside data processors using RS-485 protocol. The method presented in this document is built based on the a normal inclinometer. Traditional inclinometer used in construction is a probe with an Inertial Measurement Unit (IMU) inside. With the inclinometer putting vertically, it is capable of measuring

the rotation of the probe along yaw and roll axis. A long wire holding the inclinometer probe while also transmit the data is connected to the probe. On this wire, there are different designs to mark the nodes that is equally distributed along the lines and with same intervals. Usually, a data processing and displacement equipment will be connected at the end of the wire to display the current data to workers.

To use a inclinometer tube on a construction site, the workers need to bring the inclinometer with them. To acquire the data, first, the workers need to put the inclinometer probe down through the buried tube and stopped the tube at each node and record each node's data for A+ and B+ as shown in Fig. 1(a). Then the workers need to pull the inclinometer up out of the tube and turns it for 180 degrees and repeat the previous process to measure the other two side A- and B- as shown in Fig. 1(b).

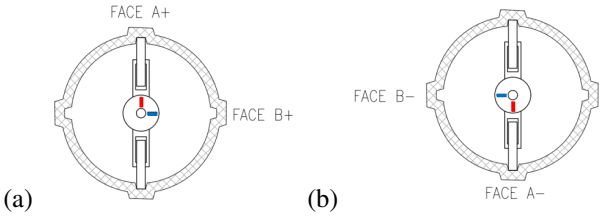

Fig. 1. Example of a figure caption.

Take A+ and A- as example, if the raw angle data acquired in degree for face A+ and A- is θ_A^+ and θ_A^-, theoretically, the following equation can be reached: $|\theta_A^+| = |\theta_A^-|$. But in reality, due to the manufacture process of a inclinometer and the positioning of the sensor inside the probe, there will be errors. The errors θ_e is calculated by: $\theta_{eA} = \frac{\theta_A^+ - \theta_A^-}{2}$ and the data can be processed as $\theta_A^{+\prime} = \theta_A^+ - \theta_{eA}$ and $\theta_A^{-\prime} = \theta_A^- + \theta_{eA}$. The same logic can be applied to face B+ and B- to get $\theta_B^{+\prime}$ and $\theta_B^{-\prime}$. As shown in Fig. 2(a), the interval between each nodes is L and the angle measured for each nodes is θ. From the geometric relationship of Fig. 2(b), the deviation from vertical i.e. the horizontal displacement can be calculate as:

$$Deviation\ from\ vertical = L \times sin(\theta) \tag{1}$$

The real displacement of a nodes on a faces is then calculated cumulatively:

$$Displacement = \sum (L_i \times sin(\theta_i)) \tag{2}$$

By getting all the nodes data for A+/A- and B+/B- faces and compare the different set of data at different time, a displace profile in respect of depth and time can be generated.

III. Problem Defining

The team start the project with several conversations with Paul Y. Engineering. During the conversations, the team realize that there are many improvement that can be made in land-movement monitoring industry. As a result the team choose to focus on this area and asked more in details.

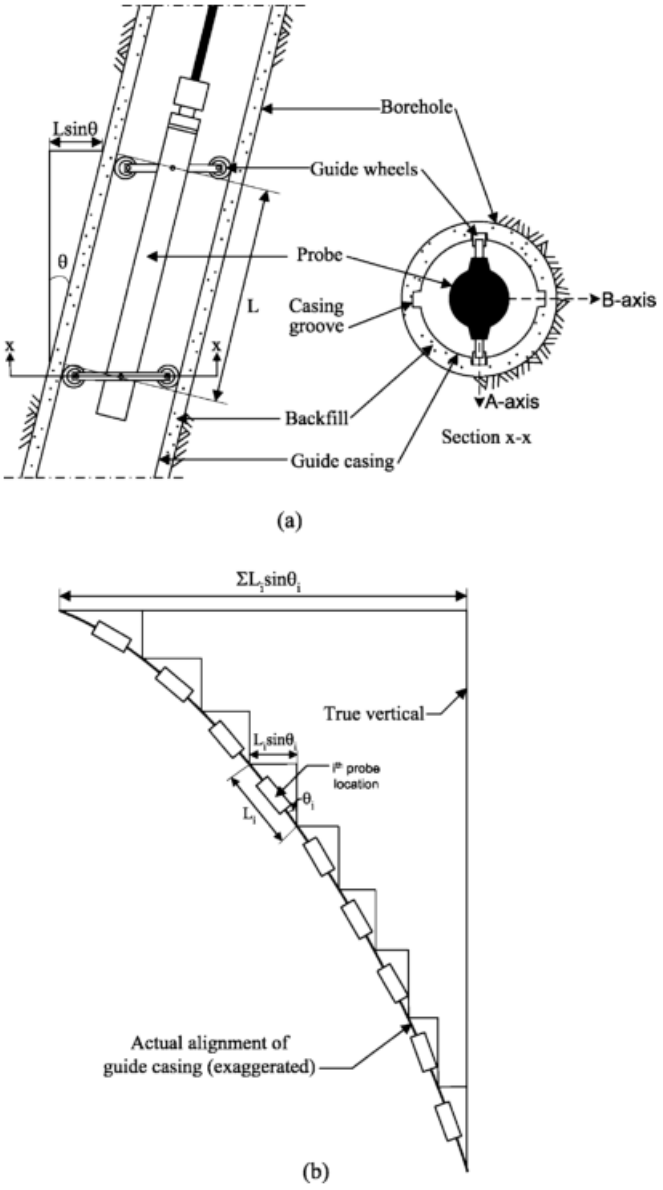

Fig. 2. a: Principles of inclinometer configuration of inclinometer equipment. b: Illustration of inclinometer operation

A. Empathize and Observation

Paul Y Engineering is a construction company that aims to provide engineering and construction solutions to its clients. We interviewed them and even went on a site visit to understand the building process and the pain points during it. One problem that they had was that they had to monitor the inclination and subsidence of the ground during the construction process to ensure that the ground had not moved a lot to ensure safety. Processes like excavating a large hole in the ground or piling to create a strong foundation for the building would exert forces on the nearby ground, which might cause instability or landslides at worse. We summarize the process of monitoring as following.

1) Choosing a location to measure
2) Digging a hole
3) Sampling
4) Assembling and advancing the case
5) Back-filling and grouting
6) Installing the inclinometer
7) Reading data from inclinometer
8) Monitoring
9) Uninstalling the inclinometer

We choose some pain points that discovered in our empathize process as our target delivery goals.

B. Problems Identified

1) Data manipulation: The normal inclinometer has cumbersome data acquisition and data processing process. Normal inclinometer is operated by workers. The workers need to carry the inclinometer probe with them and go to work on site. The data is usually recorded manually on papers and transfer into an excel file later for data processing. while the data processing is done also by excel and output into a PDF file for future inspection. Also, human interaction with the machine leaves large uncertainty for the existence of human error.

2) Time and frequency: The using method of normal inclinometer takes time. It takes two to three workers around 20-40 minutes to measure a inclinometer hole. And due to short of labor, the workers only measure one hole for around once to twice a month which this report argues that it is not frequent enough for land movement monitoring.

Under the above observation, the team would like to make the ground monitoring process real-time while providing a better user experience compared to existing solutions.

IV. Literature Review

After the problem definition, the team looks for existing similar product in the market. The team find two major existing product which is not widely used.

A. Digital Inclinometer System

C17-PRO Vertical Digital Inclinometer System is an inclinometer system integrated with an information system [3]. The advantages include automatic data processing, automatic data uploading, and it can perfectly fit in the current system. However, it still requires a human worker to operate, so it is hard to achieve real-time monitoring.

B. ShapeArray

ShapeArray (SAA) is an array of rigid segments separated by joints that can move in any direction [4]. MEMS gravity sensors placed in each segment measure the tilt in two directions. Processors transform each joint's position (e.g., X, Y Z) to produce the change of shape of the whole tube.

V. Proposed Idea

The project proposed an Intelligent Real-time Land-movement Monitoring System (IRLMS) with two measuring method. One is the Smart Inclinometer (SInc) method and one is the Meter In a Tube (MIT) method.

A. Smart Inclinometer (SInc)

In the previous session, the discussion mainly developed around the workers. The idea of SInc is to replace the workers with robotics devices. A SInc is a stationary device that sit on the top of each inclinometer tube. Inside the a SInc contains mechanical and electronic devices that can control the movement of a normal inclinometer. The machine can operate at anytime, allowing more frequent and flexible inspection. The machine will be able to collect the data, process the data and send the data to the cloud server. The workers are able to access the data through online website. The back end of the server will analyze the data collected, generate reports and issue alert if needed. Human Machine Interface (HMI) is also built inside the machine to allow workers to control the machine on site if needed.

B. Meter In a Tube (MIT)

Unlike inclinometers, where the inclination at different depths of the tube is measured by an IMU and chained together to form the shape of the tube, MIT works by measuring the curvature of the tube at regular intervals, and subsequently reconstructing the shape of the tube using the acquired curvature data. Sensing of the tube curvature is done using the strain gauge. Strain gauges are sensors that respond to strain. Simply put, the resistance of a strain gauge varies with its length. When attached to the surface of a tube, the bending of the tube causes part of its surface to become elongated, and another part to be compressed.

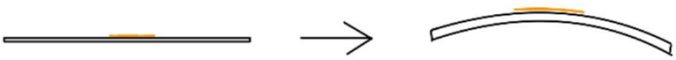

Fig. 3. Working Principle

If a strain gauge is attached to the surface, the amount of elongation or compression can be sensed. Since the strain experienced by the strain gauge is dependent on the bending curvature (the inverse of bending radius) of the tube at that location, by attaching strain gauges at regular intervals on the tube, the curvature at different points of the tube can be sampled and later used to reconstruct the shape of the tube.

VI. The Smart Inclinometer (SInc) Method

A. Methodology

SOLIDWORKS was used for mechanical design. The machine prototype is built using common manufacturing material and process including aluminum profile, Laser-cut, CNC and 3d-printing based on the CAD drawn.

The Embedded System is divided into four parts: Low-Level subsystem, Control subsystem, Communication subsystem, Host subsystem. Low-level subsystem refers to the hardware, operation system and some basic tools. Control subsystem contains the communication between sensor and actuator

and relevant control algorithms. Communication system part discusses the design and implementation of communication protocol between host and chip. Host subsystem will cover some details about the host program running in Mini-PC for controlling the machine.

QT creator. was used for user. interface design. The on site user interface is built using qt5. To communicate with lower level subsystems. The on site user interface is deployed in the Robot Operating System (ROS) system in the mini PC. The data is transmitted through ROS topic and ROS node. This setting would make data. communication between front end, mini PC , and lower level subsystems easier and more independent to other subsystems.

The online user interaction prototype is a website built using HTML, CSS, JavaScript nodeJS and expressJS. For quick prototyping purpose, the website is deployed locally on the mini-PC inside the machine. The same mini-PC also acted as a host computer controlling the machine, this setting make data communication between website, host computer and client easier. In real deployment situation, the website should be on cloud server and the mini-PC will need to communicate and exchange data with the cloud server through cellular network.

B. Details of Design

1) ***Mechanical design****:*

This section will explain in details the mechanical design of the SInc prototype. This document stress that the prototype is different from a real deployable product. The mechanical part of the SInc consists of structure, casing, depth control mechanism, rotation control mechanism, HMI and electronics.

The structure is built using $20mm \times 20mm$ aluminum profile, forming a stable aluminum structure for holding all the mechanism inside. Four adjustable support is added at the bottom to allow height adjustment and adapt to uneven earth surface.

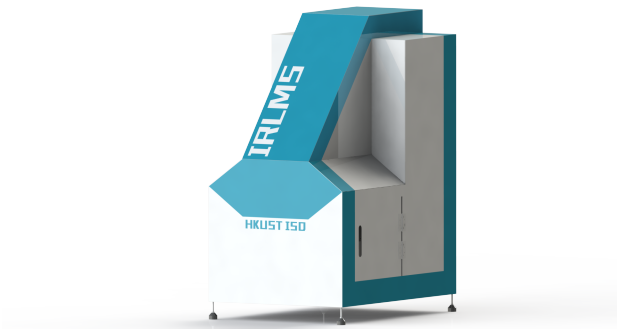

Fig. 4. Casing rendering

The rendering of the case is shown in Fig. 6. The casing is built using $0.8mm$ white polyvinyl chloride (PVC) board with heat bending process. The casing is separated to different part and the PVC board is cut into shape first and then bend into desired 3-D geometry. Different 3-D PVC board is connected together and connected to the structure using Velcro allowing easy assemble and disassemble. The casing is painted to make it more aesthetic.

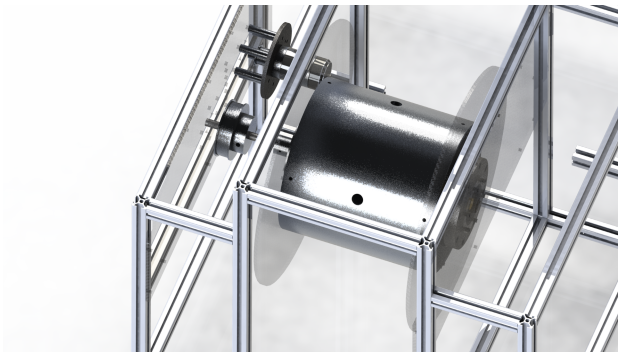

Fig. 5. Depth control mechanism rendering (Wire coil integration) (some components is hided or turned transparent)

The depth control mechanism includes a motor, a wire coil integration, a capacitive proximity switch, a color sensors. The depth control working principle is using the color sensor to detect the color mark on the inclinometer wire (white marks with dark blue wire) while each mark is separated equally and represent each node where the inclinometer will stop and measure the data. An additional capacitive proximity switch (or metal detector) is used for initializing the position of the inclinometer, making sure that the machine can get the inclinometer back to the zero position. The wire is redirected by two pulleys and into the wire coil integration. The wire coil integration is a common wire coil with a transmission connecting part on one side and a electrical slip ring on the other side. The integration is connect to the structure on the slip ring side using cross bearing. The slip ring allows the transmission of power and electrical signals from a stationary to a rotating structure. In this scenario, the rotation structure is the wire coil and the stationary structure is the electronics. The slip ring allows constant rotation while keeping the wire untangled. The transmission system is a synchronized wheel mechanism. The driving (motor) and driven (coil) wheel ratio is $1:3$ reducing the required force for the motor by $\frac{2}{3}$. The motor used in this prototype is DJI RoboMaster M3508 Gear Motor. The max continuous torque of the motor is $3N \cdot m$ providing a $9N \cdot m$ force on the coil axis. The theoretical force this machine can provide to the inclinometer probe is $9kgf$. The inclinometer probe goes down under ground using gravity and goes up back using the force provided by the motor. The motor is controlled by PID therefore can control the movement speed of the probe.

The rotation control mechanism includes a holding structure, alignment mechanism, two capacitive proximity limit switch and transmission system. The holding structure is a short segment of inclinometer (In-machine Inc tube) surrounded by aluminum-tube structure. The inclinometer probe is stored inside the In-machine Inc tube at initial state and will be put down under the ground by depth control mechanism if needed. The holding structure is connected to the machine structure by cross bearing. The alignment mechanism is 3

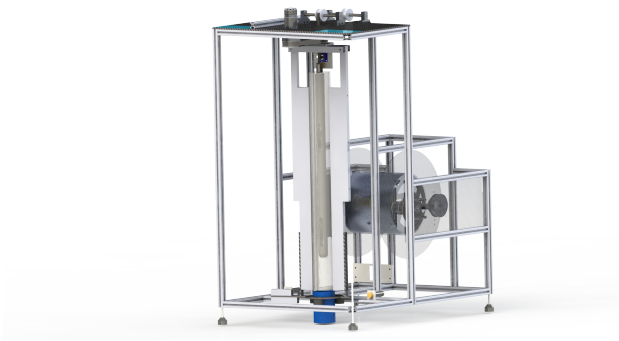

Fig. 6. Rotation control mechanism render (some components is hided or turned transparent)

equally separated wheels that connected to the holding structure and align the In-machine Inc tube to the inclinometer tube buried under the ground. The limit switch is two capacitive proximity switches limiting the rotation motion within 0 to 180 degrees. The transmission system is a synchronized wheel mechanism. The driving (motor) and driven (coil) wheel ratio is $1:1$. When the inclinometer need to change direction for 180 degrees, the motor will spin until the capacitive proximity switch is triggered.

The HMI is a touch screen normally protected by a cap on the top. When using, the workers need to disassemble the cap. The touch screen display a interaction interface from the mini-PC allowing workers to send command to the machine. The electronics consist of a power supply, a STM32 main board, several ESCs controlling the motors. The power supply is a 300w transformer tranforming 220V/380V power supply to 24V/12V supply. The board used in this prototype is DJI RoboMaster Development Board Type A.

*2) **Embedded System**:*

This section will present the design detail of embedded system part of SInc, including Low-Level System design, Control System design, Communication System design, and Host System design.

Low-Level System Design

The most used OSs (Operation System) are Windows and Linux. Both are not RTOS (Real Time Operation System). Which mean a request may be suspended for tens of, even hundreds of milliseconds. While a delay of motion execution may lead the whole system to be invalid. So, it is impossible to use a mini-PC with Linux system or Windows system to control the whole machine. For this reason, we adopt a STM32 chip with a RTOS running on it as low-level control core. All the control algorithms are deployed in this chip. And the mini-PC will communicate with low-level core for data collection, commands execution and error report via USB (Universal Serial Bus).

FreeRTOS provides us an easy way to run different tasks at the same time and lots of mechanism for control threads. We deploy FreeRTOS as our embedded operation system since there are many tasks should execute coordinately in our system. By using FreeRTOS, initialization action and routine can be separated, and we could suspend a task if necessary. The introduction of RTOS brings potential misuse of thread which leads to system stalls or out of control. To monitor the whole embedded system, SystemView, a low-level library for monitoring system status, is used. SystemView provides us a GUI (Graphic User Interface) that can visualize detail information, such as running time of threads and triggering time of interrupts, about the system that is monitored.

In the low-level system, we equipped two motors, one for controlling the depth of the inclinometer, another one for controlling the rotation of the inclinometer. We also conduct some experiments to choose sensors for controlling two motors works accurately. The final choices of sensors are: three approaching sensors, one grayscale sensor and two encoders embedded inside the motors. The details about usage of sensors and controlling actuators will be presented in next subsection.

Control System Design

The main control tasks in SInc are rotating the inclinometer to correct orientation and insert inclinometer to the right position. For clarity we name the rotating inclinometer to correct orientation as direction control and name inserting task to certain position as depth control. Both motions are done by controlling M3508 brushless motors via C620 ESC (Electronic Speed Controller). C620 ESCs support two different protocols. One is PWM (Pulse Width Modulation). Under this mode, we hand over all the motor control task to ESC and input PWM wave to indicate the target rpm. It is convenient to use PWM mode, but we cannot control the motor precisely. To control motor accurately, we choose another control mode, CAN (Controller Area Network) mode. Under CAN mode, C620 ESC will report some basic information, including, torque current, rpm, and encoder data via CAN bus. And STM32 can control the torque current by sending commands via CAN bus.

The target it to control the depth or direction of inclinometer, which is almost proportional to the total rotation angle of rotor. To reach the control target, we need an algorithm to use torque current to reach target position. We adopted PID (Proportion Integration Differentiation) algorithm, a popular feedback control algorithm in industry. A motor is a highly nonlinear system, while PID is a linear control algorithm. Use PID directly may not get a good performance. To solve this problem, we use serial PID, which input the output of higher level PID to lower level PID. In SInc, we design two level serial PID. First level, named Position PID, inputs target position and outputs target velocity. Second level, named Velocity PID, will input target velocity and output target torque current. The final commands are sent via the CAN bus, and we make an assumption that the C620 ESC can execute commands immediately and its control frequency is far higher than our command generation frequency, which is set to 1kHz. As a feedback control algorithm, PID requires sensor data as feedback data to rectify the input. We use the encoder data reported by C620 ESC as feedback data directly, since both velocity and position data has been filtered by algorithms

embedded inside the C620 ESC.

Tunning of PID parameters without modeling system highly depends on experience. In order to get practicable parameters that adjust response of system to satisfy requirement, we apply Ziegler-Nichols Method, a heuristic method, to tunning PID parameters. The final values of parameters are listed below.

		Rotation	Depth
Postiion PID	P	20	456
	I	0	26
	D	10	0
Velocity PID	P	190	456
	I	950	900
	D	285	5.7

Fig. 7. PID parameters

To detected if the inclinometer reaches target position or direction, we install a grayscale sensor and three approaching sensors. All of them are digital sensor, which only output 5V and 0V to indicate triggered or not. When the sensor reaches the threshold, the output signal may bounce. That may introduce some errors since the inclinometer is not in the right position or direction. Therefore, we need to design a method for sensor debouncing. The basic idea for debouncing is to detect the triggered time, and we only recognize a signal last longer than a certain time as triggered signal. We implemented this method via software timer provided by FreeRTOS since the real time requirements is not strict.

Communication System Design

SInc consists of GUI for users to control the whole machine, while the actuators are drove by STM32. So, we need to exchange data between Mini-PC and STM32. To achieve this goal. We design a communication protocol for data exchange. The details about implementation of communication protocol will be presented after demonstrating the protocol design and the host program running on Mini-PC will be presented in next subsection.

A simplest protocol is to assign different bit different meaning and we encode the command. For example, we let first byte to always be 0xFF for indicating the start of commands. The second byte indicates the target position, the third byte indicates the target direction. By using this fix length frame to exchange data, we can exchange data easily. But the information entropy of this kind of protocol is too low. In previous example, if we want to change the position only, the third byte will become meaningless. To solve this problem, we design a variant length frame. The whole frame contains two sub-frames, header frame and body frame. header frame contains a start byte, a protocol version identifier byte, a command identifier byte, a message identification byte, a message length byte, and a CRC-8 (Cyclic Redundancy Check - 8) check byte. The body frame contains the message stream and two bytes of CRC16. By reading the message length and command identifier in header frame, receiver can decode the message can execute the commands. The CRC bytes are used for error detection, receiver can dispose the error message by checking the CRC bytes. But the sender does not have information about this error and re-transmit can be invoked. For data integrity consideration, we require receiver to send back an acknowledgement frame back to the sender for indicating the success of communication.

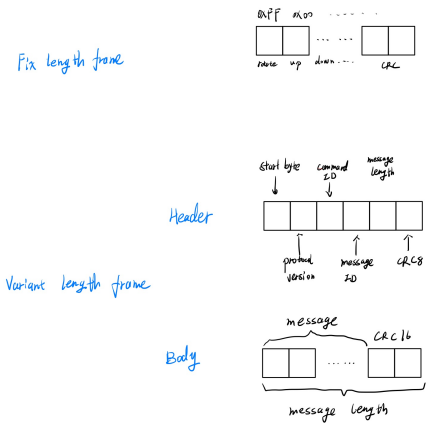

Fig. 8. Frame structure

To implement the protocol mentioned above. We use HAL (Hardware Abstraction Layer) library provided by ST company. The portability of HAL library enables us to migrate all low-level code to another chip easily. The HAL library allows us to use three different ways to receive UART (Universal Asynchronous Receiver/Transmitter) signal: blocking receive, interrupt receive, and DMA (Direct Money Access) receive. When the transmit frequency is high, blocking receive may accumulate time unalignment errors. After some messages, the communication may fail due to time displacement. Interrupt receive can solve this problem, since receiving process are done by hardware concurrently. But in our case, our frames have variant length, and receiver can only get the length of body frame by decoding the header frame. To receive the whole frame, two interrupts are needed. First for receive and decode header frame, then start second interrupt to receive body frame. However, it takes a few microseconds to handle the first interrupt. The latency leads to the receive error of body frame. To solve this issue, we combine the DMA receive and interrupt receive. A large enough buffer, it is set to 261 bytes in our case, is allocated for DMA to store all bytes received. And we setup an interrupt that is triggered when the UART turn back to idle mode. DMA guarantees the success of receiving all data, while interrupt helps invoke code which handles the data. This method has a disadvantage, that only one command can be handled. But this disadvantage can be ignored since we require receiver to send back an acknowledgement frame.

Host System Design

The host system is designed to communicate with low-level core for collecting data and errors reports form low-level core. To solve the IO (Input/Output) compatibility issue, we use

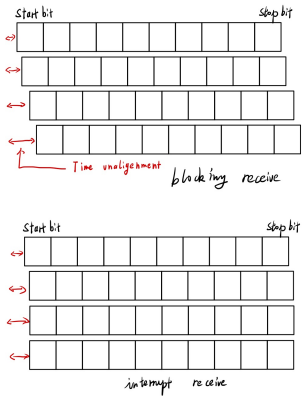

Fig. 9. Blocking receive Vs Interrupt receive

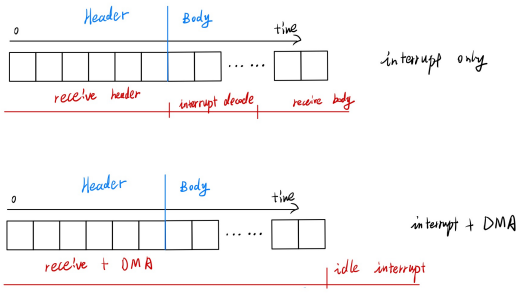

Fig. 10. Interrupt only Vs Interrupt with DMA

an CH340G chip to covert USB signal to TTL (Transistor-Transistor Logic) signal. To driver the serial port, we use an open-source library called serial [5]. The basic workflow of host system consists of five steps: 1. Host system get input from user. 2.Host system covert user input into commands and send via serial 3. Wait for acknowledgment frame. 4. Resend if acknowledgment frame is not received. 5. Report status of machine to user.

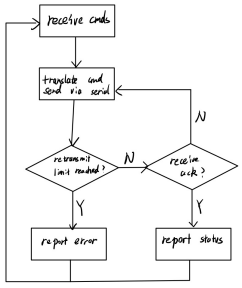

Fig. 11. workflow of host

We provided a website GUI for user to visualize all data. To reduce the works of transferring data from raw data to another data structure that can be read by website, we store all data in JSON (JavaScript Object Notation) file. For generating JSON file, we choose an open-source library called configor [6].

*3) **On site user interface**:*

The on site user interface is designed for workers on site to maintain the machine and record data from the inclinometer,including nodeID, depth,slope in X and Y directions and returning the state of machine. It also provides simple functions including move up/down the inclinometer, rotate by 180 degrees, measure and connection check.It also provides integrated function :

1) reset function will set the machine to original status
2) auto function will let the machine perform a complete measurement

The basic workflow of the user interface system consists of five steps:

1) system gets input from the frontend.
2) system convert input into commands and publish on ROS system
3) wait for acknowledgment
4) resend if acknowledgment is not received
5) subscribe the machine state topic

*4) **Online user interface**:*

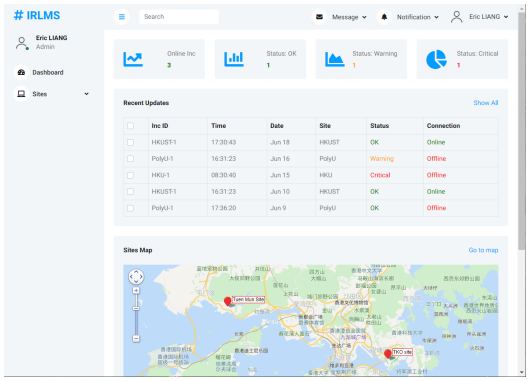

Fig. 12. Dashboard of online interface

As shown in Fig.12, the index page of the website is a dashboard detailing the summary of the whole system including amount of SInc online offline, amount of SInc reporting OK status, WARNING status and CRITICAL status, All the site available and their location on map.

The users can access different site by going to the site page as shown in Fig.13. The site page will display all the SInc in the site and their basic information, latest update time and current status. The detailed position map of each inclinometer in the site will also be shown in this page.

The users can see each inclinometer in details by clicking into different inclinometer page on site page. Fig.14 and Fig.15 is appearance of the inclinometer page. The users can see all necessary information of this inclinometer on inclinometer page including all the data measured, the analysis and graphs of the data. The users will also be capable of generate and download reports from this page.

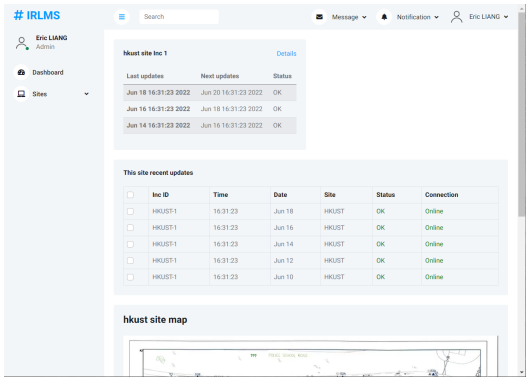

Fig. 13. Site page of online interface

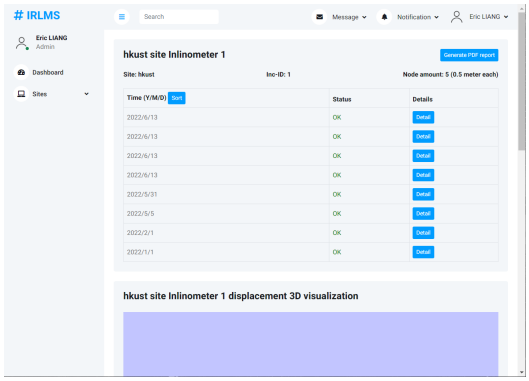

Fig. 14. Inclinometer page of online interface - upper part

The users are also capable of viewing raw data and process data for a certain measurement as shown in Fig.16. By clicking into different set of data on inclinometer page, raw angle data, processed horizontal displacement data, processed cumulative displacement data, processed reference displacement data will all be shown.

*5) **Operation**:*

The SInc run automatically in normal situation. Every period of time, it will run a set of command and the following movement will be made:

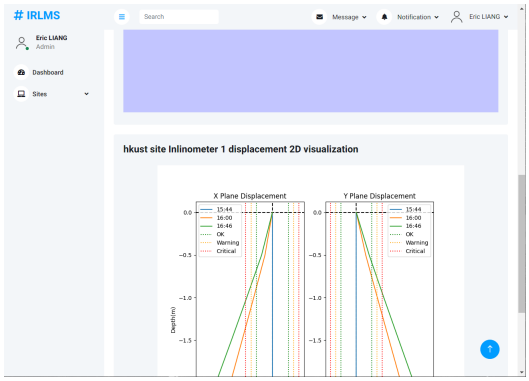

Fig. 15. Inclinometer page of online interface - lower part

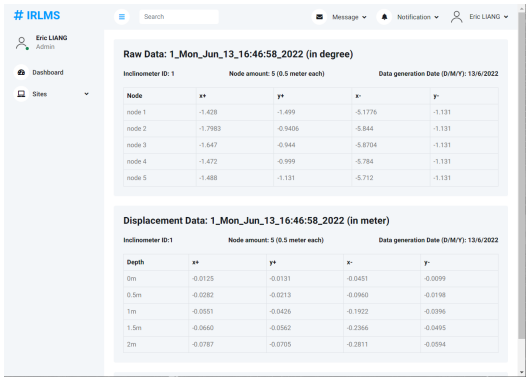

Fig. 16. Raw data page of online interface

a) Initialization: The machine initialize itself by pulling the inclinometer probe up until the depth control proximity switch is triggered. Then the SInc will put the probe down until it reach the 0^{th} mark on the line. At 0^{th} mark, the inclinometer is inside the machine and no data is collected. Then the SInc will rotate the inclinometer towards 0 degree until the 0 degree proximity switch is triggered. The initialization is finished.

b) 0 degree Measurement: The SInc will put the probe down and stopped at each node to collect the data. At each node, the color sensor will detect the mark and the depth control motor will stopped. When the last node is reached, SInc will pull the probe back to 0^{th} mark. The rotation motor will then rotate turning the probe towards 180 degree until the 180 degree proximity switch is triggered

c) 180 degree Measurement: The SInc will put the probe down and stopped at each node to collect the data. At each node, the color sensor will detect the mark and the depth control motor will stopped. When the last node is reached, SInc will pull the probe back to 0^{th} mark while a file is generated storing all the raw degree data collected. The rotation motor will then rotate turning the probe towards 0 degree until the 0 degree proximity switch is triggered.

d) Finishing: All the motors will be locked and the SInc will wait for next measurement while the data is processed and sent to cloud and can be access either on site or online.

For the workers working on site, the interface allow them to see the current situation and errors of the machine and control the machine to go to certain nodes to check a specific data.

C. Testing set up

Due to the pandemic, the team have limited resources and less accurate means to perform experiment. Therefore, larger errors is accepted in this document.

As shown in Fig. 17, the testing environment is a 3 meter high platform built between the empty space of a stair case by aluminum profile and wooden board where a 3 meter long inclinometer tube is mounted on the wooden board simulating the tube buried underground. By observation, the platform is not perpendicular to the gravity direction, therefore the tube is not vertical at its initial state. The machine is placed as

Fig. 17. Testing environment

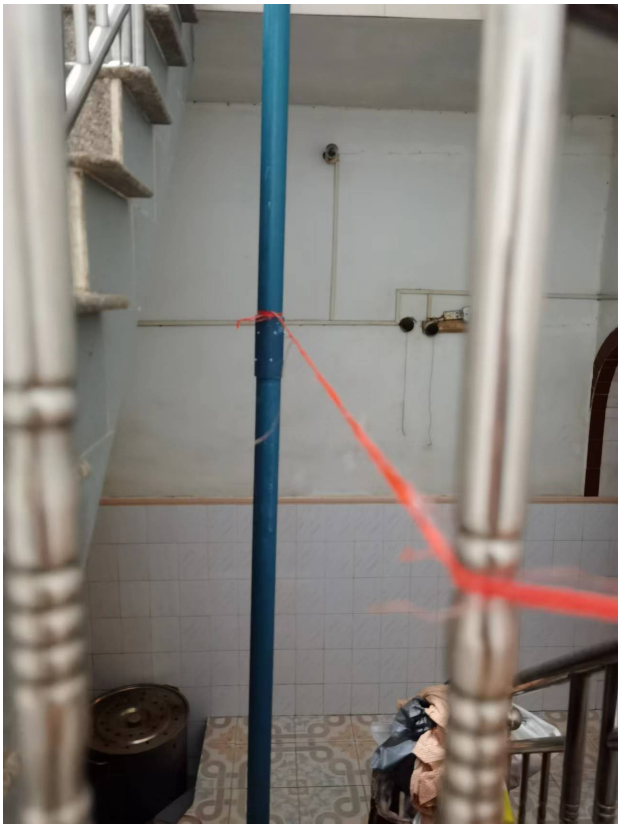

Fig. 19. Dragging method

shown in Fig. 17 and the coordinate is defined as Fig. 18 (for reference Fig. 17 is shot from x- direction).

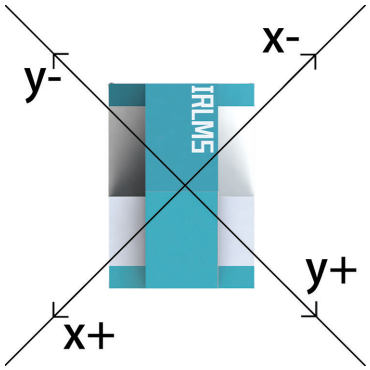

Fig. 18. Testing environment coordinate system

The testing tried to simulate the process of a land-movement towards the x- to y+ 45° direction. As shown in figure a wire is connected to the tube at 2m position and drag towards the desire direction. As shown in Figure. 19, the dragging distance is measure using the wire length. The dragging distance is measured by band tape. The team member pull the wire and after measurement tied the wire to the stair case hand rail to make it stable. This may result in length uncertainty, since the operation and tying method may result in reduction of dragging distance.

Furthermore, slight vibration of the inclinometer tube is observed during the experiment. The team argues that it might affect the acquired data, increasing its uncertainty. But in real life implementation, soil is surrounded tightly and no vibration will be generated.

The testing is performed on Jun 13th. The baseline is recorded at 15:44. Then the tube is dragged towards the x- to y+ 45° direction for 0.08m and the data is recorded at 16:00. At last the tube is dragged towards the same direction for 0.1m and the data is recorded at 16:46.

D. Testing Result

The raw data received from the inclinometer is angle data, using the approach explained in previous sections, the horizontal displacement, cumulative displacement and reference displacement to the baseline of different time and different nodes can be calculated as shown in TABLE I. TABLE II shows the displacement profile along face x, face y and dragging direction face of different nodes at different time.

The data in TABLE II ”Displacement Profile along x- to y+ 45°” shows that at 16:00, the tube is dragged towards the x- to y+ 45° direction for 0.0702m and at 16:46, the tube is dragged towards the same direction for 0.0922m. The actual data collected compared to expected data has an 12.25% and 7.80% error. As mentioned in previous section, there are uncertainty and errors in this measurement, therefore this document argues that these errors are acceptable.

TABLE I
MEASURED DATA OF HORIZONTAL DISPLACEMENT, CUMULATIVE DISPLACEMENT AND REFERENCE DISPLACEMENT TO INITIAL STATE

in m	Hor. Disp.		Cum. Disp.		Ref. Disp.	
Depth	**x**	**y**	**x**	**y**	**x**	**y**
Jun 13th 15:44						
0.5000	-0.0167	-0.0264	-0.0167	-0.0264	0.0000	0.0000
1.0000	-0.0165	-0.0261	-0.0333	-0.0524	0.0000	0.0000
1.5000	-0.0155	-0.0264	-0.0488	-0.0788	0.0000	0.0000
2.0000	-0.0142	-0.0268	-0.0630	-0.1056	0.0000	0.0000
2.5000	-0.0143	-0.0270	-0.0772	-0.1326	0.0000	0.0000
Jun 13th 16:00						
0.5000	-0.0250	-0.0155	-0.0250	-0.0155	-0.0083	0.0109
1.0000	-0.0292	-0.0126	-0.0542	-0.0281	-0.0210	0.0244
1.5000	-0.0286	-0.0126	-0.0829	-0.0407	-0.0341	0.0381
2.0000	-0.0274	-0.0130	-0.1102	-0.0537	-0.0473	0.0519
2.5000	-0.0273	-0.0134	-0.1375	-0.0671	-0.0602	0.0656
Jun 13th 16:46						
0.5000	-0.0288	-0.0115	-0.0288	-0.0115	-0.0121	0.0149
1.0000	-0.0333	-0.0090	-0.0621	-0.0205	-0.0289	0.0319
1.5000	-0.0328	-0.0091	-0.0949	-0.0296	-0.0461	0.0493
2.0000	-0.0316	-0.0093	-0.1265	-0.0389	-0.0636	0.0668
2.5000	-0.0314	-0.0099	-0.1579	-0.0487	-0.0807	0.0839

TABLE II
DISPLACEMENT PROFILE FOR FACE X, FACE Y AND FACE X- TO Y+ 45°

Displacement Profile for Face x			
In m	**Jun 13th**		
Depth	**15:44**	**16:00**	**16:46**
0.5000	0.0000	-0.0083	-0.0121
1.0000	0.0000	-0.0210	-0.0289
1.5000	0.0000	-0.0341	-0.0461
2.0000	0.0000	-0.0473	-0.0636
2.5000	0.0000	-0.0602	-0.0807

Displacement Profile for Face y			
In m	**Jun 13th**		
Depth	**15:44**	**16:00**	**16:46**
0.5000	0.0000	0.0109	0.0149
1.0000	0.0000	0.0244	0.0319
1.5000	0.0000	0.0381	0.0493
2.0000	0.0000	0.0519	0.0668
2.5000	0.0000	0.0656	0.0839

Displacement Profile along x- to y+ 45°			
In m	**Jun 13th**		
Depth	**15:44**	**16:00**	**16:46**
0.5000	0.0000	0.0136	0.0192
1.0000	0.0000	0.0322	0.0430
1.5000	0.0000	0.0512	0.0675
2.0000	0.0000	0.0702	0.0922
2.5000	0.0000	0.0891	0.1164

Each measurement cycle (go down and go up twice) takes around 3 minutes. This means the data refreshing rate can go high up to 480 times per day, much better than the normal inclinometer solution whose refresh rate is 2-3 times a week.

In experiments, the data is shown on the website immediately which allow online data access, process and manipulation. Figure.20 shows the displacement visualization of x plane and y plane.

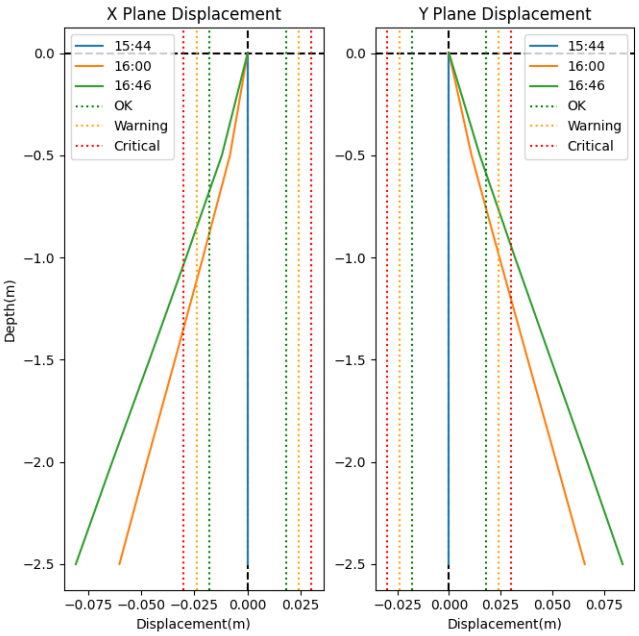

Fig. 20. Data Visualization

E. Potential Improvement

During the experiment, the team found that there are several improvement can be made to make SInc better.

The motor used can be improved. The DJI RoboMaster M3508 gear motor is a brush-less motor with planetary gear reduction gearbox. While it perform well enough for prototyping purpose, a high torque testing is performed and the temperature of the motor goes up quickly under high stress which is not ideal for long term service. Therefore, A motor with a worm gearbox is better in this situation. The worm gear motor is capable of self-lock itself when the motor is not spinning, avoiding the high torque situation.

In current solution, we use color sensor to detect color marks on inclinometer wires to determine the depth. In testing and experiments, the team found this method unreliable and may be related to surrounding temperature and humidity. Absolute encoder or pure physical marks (ex: physical marks on wires trigger physical sensors) may be a better solution then color sensors.

VII. The Meter In a Tube (MIT) Method

A. Methodology

B. Details of Design

*1) **Mechanical Design**:* The mechanical design part of MIT consists of three main parts, attaching sensors into the tube, segments connector design, and the test rig. The prototype is made in half-scale to allow for easier prototyping and testing.

Attaching sensors into the tube - prototype making

Previously, a prototype was made where the sensors are adhered to a flat plate, and we were able to visualise how it deforms digitally. After testing it on a flat plate, we then proceed to test it on a tube that has a curved surface.

There are different methods to attach the sensors to the tube, adhering them to the outer surface of the tube, embedding them in the middle of the tube wall, and adhering them to the inner surface of the tube. Theoretically, the most ideal position is to embed them into the middle of the tube wall so that the sensors are fully enclosed and protected from direct impact or moisture.

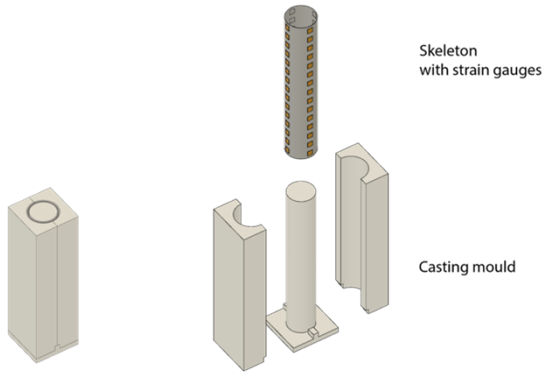

Fig. 21. Closed and exploded view of the casting setup

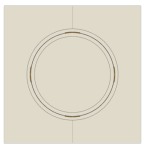

Fig. 22. Top view of the casting setup

To make it, moulds are made that have the negative shape of the tube and a skeleton will be inserted into the middle of the negative section of the mould as seen in Fig.22. The skeleton will be responsible for the alignment of the sensors and to hold them into place during the moulding and casting process. Existing tubes that are used for land monitoring are typically made from PVC and ABS with a diameter of 60mm. Resin with mechanical properties similar to existing tube materials is chosen and is poured into the mould to fill and enclose the sensors in between. Relative materials properties are shown in following table

Material	Young's Modulus (psi)	Flexural Modulus (psi)	Shrinkage (%)
PVC	400,000	188,000	0.4
ABS	260,000	240,000	0.6
Smooth-on Task 2 Resin	290,000	288,000	0.5

However, this method would result in a very long making and waiting process – it takes a lot of work to make one tube and requires a day to fully cure. In addition, the wires of the sensors cannot be routed perpendicular to the surface of the tube so they can only be routed along the length of the tube. Therefore, the wires have to be extended and exit from the ends of the tube which would increase the duration of manufacturing.

To quickly get an initial understanding of the strain gauges when they are attached on a tube, we decided to directly adhere them to the outer surface of the tube. There are two advantages of doing this. Firstly, since the sensors are stuck on the outer surface, sticking them to the tube is a straightforward process. Secondly, the sensor and wires are exposed and reachable which eases testing and troubleshooting.

Prototype 1

The first prototype (Prototype 1) is a 1-meter-long tube with 100mm sensor spacing in one line – resulting in 10 sensors in total. 100mm spacing was decided to quickly get an understanding of how the sensors behave and see if we can reconstruct the shape of the tube digitally with the algorithm that we have written. There are 5 steps in total when creating Prototype 1, cutting the tube to the desired length, drawing a straight line along the tube, measuring and marking the 100mm spacing, drawing circumference lines at the markings along the tube, and sticking the strain gauges at the intersections of the lines.

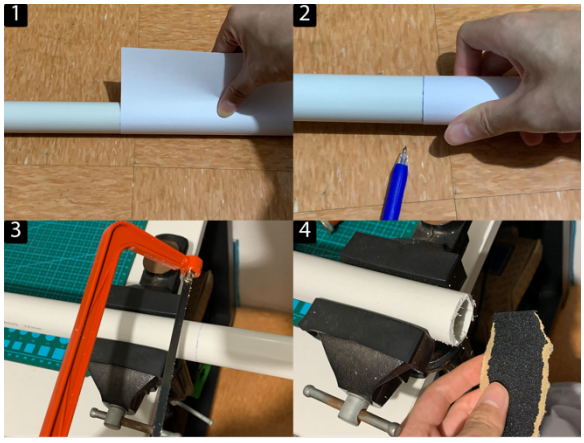

Fig. 23. Steps to cut the tube into 1 metre

To cut the tube to the desired length, 1 meter is measured and marked with a dot on the tube. However, the cutting process might lead to a slanted cut which would make the tube have different lengths at different positions. To achieve a

straight cut, a strip of paper is wrapped around the circumference of the tube. When the edges of the paper align, it provides a guide that guarantees a line that is perpendicular to the length of the tube. The tube is secured on a vice clamp and a hack saw is used to cut the tube. During the cutting process, the cut should follow the line drawn previously. If the cut is slightly angled, which means there is still some material outside the drawn line, sandpaper is used to sand them away to achieve a straight and smooth cut.

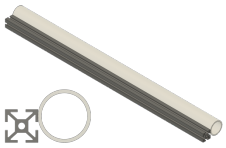

Fig. 24. Line drawing setup V1 with the cross-section on the left

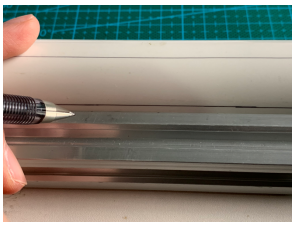

Fig. 25. Drawing lines with line drawing setup V1

To draw a straight line of a tube, a similar length 2020 aluminium extrusion is placed next to the tube and used like a ruler as seen in Fig.24 and 25. This allows the tube to rest against the extrusion and not move around while drawing. A ballpoint pen is used and glided along the edge of the extrusion to create a line. However, this setup heavily depends on the straightness of the tube and aluminium extrusion which will be addressed in the next prototype.

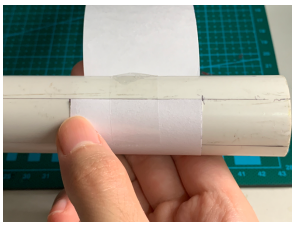

Fig. 26. Drawing the circumference line at the marked location

The spacing is measured and marked by placing a flat ruler onto the previously drawn line. Every 100mm is marked with a dot on the line. A circumference line is then drawn using the aforementioned paper wrapping method to create an intersecting cross on every location the sensor has to be stuck on since it will be used to align the sensor in the correct direction.

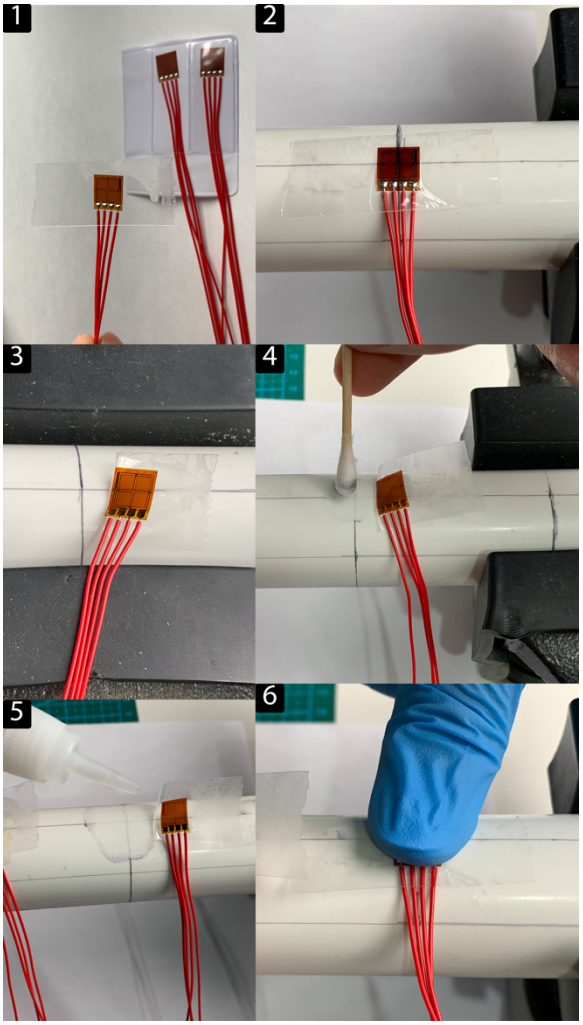

Fig. 27. Steps to stick strain gauge sensors to the tube

The sensor sticking process is shown in Fig.27.Firstly, the sensor will be first stuck on a piece of tape to prevent contaminating the sensor surface with dirt and oils and to allow the sensor to be aligned and maintain its aligned position. When looking closely, the sensor has alignment arrows on the top, bottom, left, and right. These arrows are then aligned to the intersecting lines drawn previously to ensure that it is at the correct location and squared with the tube. The sensor is then partially opened, and the tube is wiped with 99% isopropyl alcohol to remove dirt and oils on it as seen in steps 3 and 4. A small amount of cyanoacrylate is placed on the surface of the tube and a finger is used to press onto the sensor for around 1 minute to ensure that it has good contact with the tube when the adhesive has cured.

Fig. 28. Prototype 1

After all these steps, Prototype 1 has been made. With it, we

were able to use it to create the first version of the algorithm to construct the curve of the tube on 1 axis.

Prototype 2

Prototype 2 is similar to Prototype 1 where only one line of sensors is adhered to the tube. But this second prototype is made to allow us to determine the optimal spacing of the sensors. Therefore, the spacing of Prototype 2 is decreased by half – from 100mm to 50mm. This allows us to place the sensors more densely and test out different spacings with the same tube – 50mm, 100mm, 150mm, and 200mm.

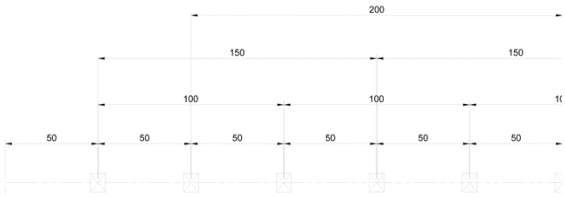

Fig. 29. The spacings available for testing

After making the first prototype, we found out that we can improve the process of drawing a straight line on the tube to improve the precision of the sensor alignment.

Fig. 30. Line drawing setup V2

Fig. 31. Updated setup drawing lines on a tube

The previous method of using an aluminium extrusion to draw lines on a tube a simple but relied on the straightness of the tube and extrusion to achieve a straight line along the centre of the tube. This second version instead takes reference of a glass surface which is much flatter than other common materials. The updated setup has a hole for inserting a ball point pen with a screw perpendicular to it to secure the pen onto the 3D printed part. The part also has two holes to mount a 22mm Delrin wheel on a bearing which allows for smooth movement along the surface. With this setup, it references the two relatively flat surfaces of the glass table to draw a straight line along the tube.

The steps for measuring, marking the spacing, drawing the circumference lines, and adhering the sensors to the tube are

similar to Prototype 1 but repeated around twice as much since the spacing has been reduced by half. To speed up the process, instead of sticking the sensors one by one, each step is done 19 times before proceeding to the next step – similar to a factory assembly.

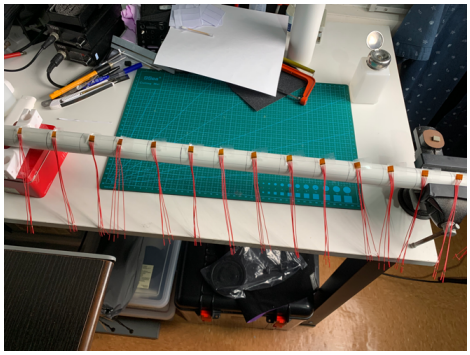

Fig. 32. Factory-style assembly

The previous prototype was exactly 1 metre long. However, the clamps of the testing rig are 50mm in total which would reduce its effective bending length by 50mm. Therefore, the tube length of Prototype 2 is 1.05 metres with 19 strain gauges in total in one line.

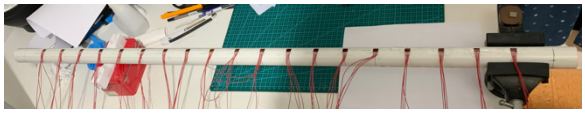

Fig. 33. Prototype 2

Prototype 2 allowed us to determine the most optimal sensor spacing by using sensors at different locations. After testing with our test setup, the most optimal spacing is 150mm and will be used to create the triplets in the next prototype.

Prototype 3

Prototype 3 begins to add sensors around the tube that are spaced 120 degrees apart. In total there are 3 sensors in one location and are called triplets. There would be triplets in every 150mm, resulting in 21 sensors in total around and along the tube.

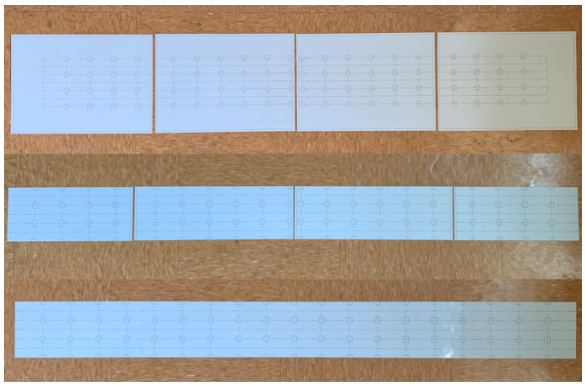

Fig. 34. Making process of the stencil

To measure and mark the triplet locations. A stencil layout is drawn in a CAD software which has the sensor spacings and the location of the triplets. The location of the triplets along the circumference is calculated by:

$$[h]Tripletlocation = \frac{2 \times \pi \times r}{3} \tag{3}$$

It is then printed in 1:1 scale on an inkjet printer. Since the tube is around 1 metre long, multiple A4-sized papers are required. They are combined and checked to ensure that their spacing is correct. The spacing is denser than 150mm since we would like to have more locations to measure with the dial indicator at the test rig. This way we can get a more accurate ground truth. This will be further elaborated in the sensor spacing test rig section.

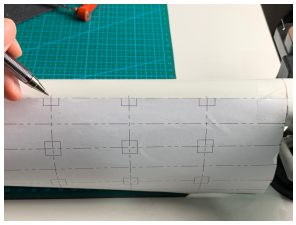

Fig. 35. Sticking the stencil onto the straight line and making sensor locations

The locations of the sensors are marked and the previous steps are repeated to draw the alignment lines and stick the sensors.

Prototype 3 allowed us to code and construct the shape of the tube in 3 dimensions as opposed to 1 dimension in the previous two prototypes.

Prototype 4

For prototype 4, after knowing the optimal sensor spacing and being able to construct the shape of the tube digitally

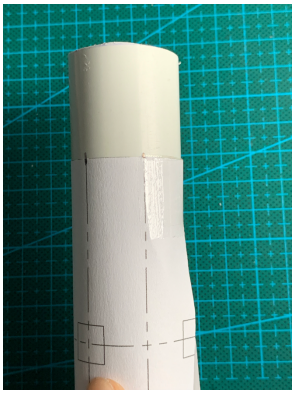

Fig. 36. Wrapping the stencil around the tube to mark 120-degrees locations

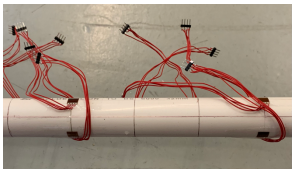

Fig. 37. Prototype 3

in 3 dimensions, we improved the prototype by adhering the sensors to the inner surface of the tube. Firstly, the sensors will be inside which will be protected by the tube instead of being exposed to the elements. Secondly, it would clean up the prototype since there will be no exposed wires outside. Sticking the sensors to the inner surface is the final form and is most similar to the initial idea of embedding the sensors into the tube.

Prototype 4.1

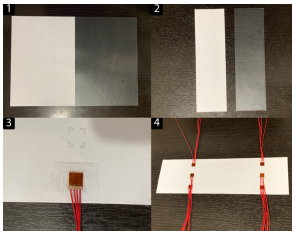

Fig. 38. Steps to stick the sensors on the film

To stick the sensors on the inner surface of the tube, it is first stuck on a piece of 0.2mm transparent PVC film. A stencil is made similar to the previous method. This stencil will be used to cut the film into the correct size. Then the stencil will be placed under the PVC film to guide the alignment of the sensors.

A new line drawer is made to further improve the accuracy of drawing straight lines on the tube. This setup has two holders with a cutout on the top to align with the marks to rotate the tube 120 degrees. The line drawer will be first rotated till the two bearings touch the tube. This ensures that the line

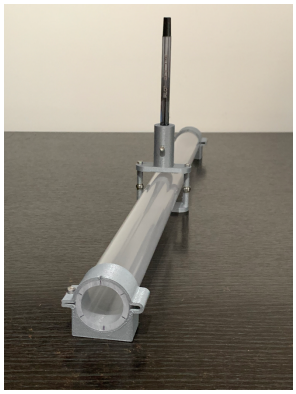

Fig. 39. Line drawing setup V3

drawn is at the centre of the tube. It is also used on a glass table since it requires a reference plane to move along.

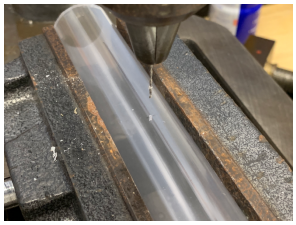

Fig. 40. Drilling holes at the sensor location

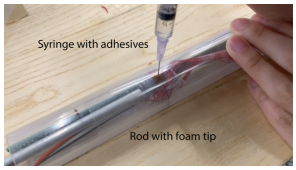

Fig. 41. Process of sticking sensors into the inner surface

To stick the film to the inner surface of the tube, 1mm holes are drilled at the location of the sensors. Cyanoacrylate adhesive is then injected with a syringe and the sensor is pushed with a long rod with a foam tip to ensure good contact. Being able to see where the sensor is inside the tube and see how the adhesive has flowed is one of the reasons we chose to use a transparent PVC tube. It would also allow the viewers to understand that it is not a normal PVC tube but a tube full of sensors and electronics.

Prototype 4.1 gave us an understanding of how to make a tube with the sensors inside. While inserting the film into the tube, creases and kinks will occur and will destroy the strain gauges. We used this information to create two more new tubes with the experience we got from it.

Prototype 4.2

After gaining the experience in making the previous prototypes, we have made our final prototype of a 1m tube filled with triplets of sensors with 150mm sensor spacing.

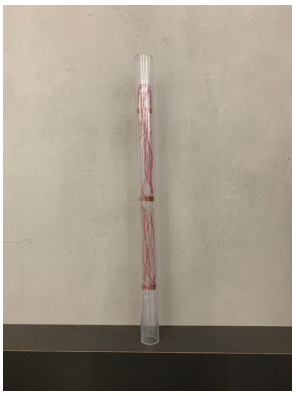

Fig. 42. Prototype 4.1

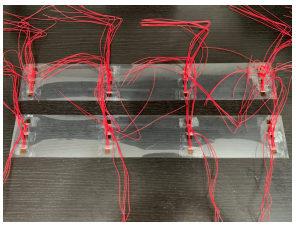

Fig. 43. Sensors adhered to the films

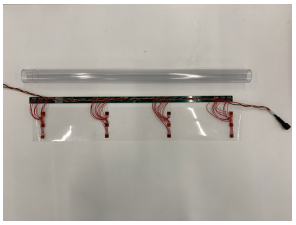

Fig. 44. Parts overview

Fig. 45. Final Prototype

Segment connector design

To connect the two segments, a connector is designed to improve assembly times while ensuring a strong and durable connection.

There are different ideas that we have thought of that would be suitable for it.

Bayonet mounts of cameras would be suitable since lenses are very similar to tubes. It is also suitable since camera lenses require correct alignment every time and require an electrical connection at the connector. However, this idea is too costly to realise, and using a different material at the connector will affect the bending and curvature of the tube.

Another method is to use snap-fit joints. This solution is great since it uses the same material as the tube and it does not require extra tools to install. However, machining the hooks for the snap-fit joints will be expensive and it is almost impossible to detach when necessary.

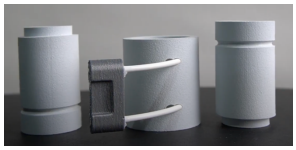

Fig. 46. Collar with cable along (middle) with the upper and lower tubes (left and right respectively)

The final method used is by cutting a circular groove at the collar and the tube. A wire is then inserted into the groove which will lock them into place. The tubes are aligned by a cut-out on the tube and a key at the inner surface of the collar.

Test rig

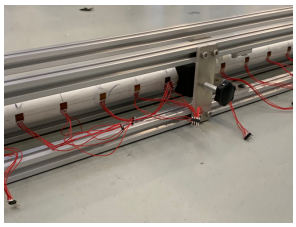

Fig. 47. Final design of the test rig

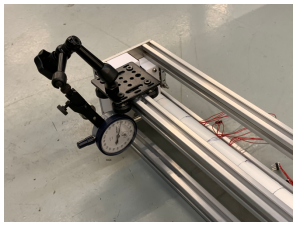

Fig. 48. Dial indicator on a slider carriage

The test rig frame is created with 2020 aluminium profiles and 5mm aluminium plates. Since it is more than a metre long, there are plates mounted along the extrusions to further increase the rigidity of the frame to prevent bending.

The tube is clamped with 3D printed parts with a layer of tennis racquet grips tapes to increase friction. Only one side is fully constrained (fixed support), and the other end is free to move coaxially (rolling support). This is to mimic how the tube will be mounted in the construction site where the bottom is fully constrained to the bedrock and the top is free to move coaxially since it is not constrained.

The pusher could be mounted at any location and any amount of pusher could be added to the test rig which increases the flexibility during testing.

To get the ground truth of the tube, a dial indicator will slide along the extrusions and measure how much the tube has actually deformed.

2) Product Design: To improve the presentation of our final prototype, a realistic 3D model is created according to it. The tube size, sensor spacing, sensor wiring, PCB ICs, and traces are all modelled in CAD software. It is then rendered in different states to show how it works and the components inside it which would act as a digital copy of the tube we have created.

Fig. 49. Two segments connected with a collar

Fig. 50. Single segment of the tube

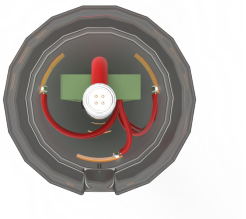

Fig. 51. Top view

3) Electronics Design:

Choice of SG amplifier IC

Fig. 52. Close-up of two segments and the cut-out for alignment

Fig. 53. Close-up of two segments connected with a collar

Although the bending of the tube results in a change in the resistance of the strain gauges, the change is miniscule and would be extremely hard to measure directly. Instead, it would be preferable to convert this change to a voltage, which can be relatively easily amplified and digitized. To do this, 4 resistors, one being the strain gauge, can be connected to form a Wheatstone bridge as shown in Figure.54. The output voltage can be described by the following equation:

$$[h]V_o = V_{EX}(\frac{R_3}{R_3+R_4} - \frac{R_2}{R_1+R_2}) \tag{4}$$

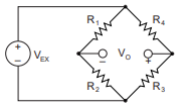

Fig. 54. Wheatstone Bridge

If R_2 and R_4 are replaced with strain gauges, any change is the resistance of the strain gauges would produce an output voltage proportional to the change in resistance. Since the change in resistance of the strain gauge is equal to the strain applied to it, multiplied by the resistance of the strain gauge, and by strain gauge dependent constant known as the gauging factor (GF). Assuming the two strain gauges are physically placed close to each other, the strain they experience would be the same, therefore the ratio between the output voltage and the excitation voltage becomes:

$$[h]\frac{V_o}{V_{EX}} = \frac{GF \cdot \epsilon}{2 + GF \cdot \epsilon} \tag{5}$$

Rearranging,

$$[h]\epsilon = \frac{2 \cdot \frac{V_o}{V_{EX}}}{GF \cdot (1 - \frac{V_o}{V_{EX}})} \tag{6}$$

Apart from strain, strain gauges also react to temperature, a change in temperature can cause a change to the resistance as well, affecting the output voltage. To compensate for this, R_1 and R_3 can be replaced with what are known as dummy strain gauges, which are strain gauges placed orthogonally to the direction of strain. This way, the strain has little effect on the dummy gauges. On the other hand, temperature affects all four gauges equally, thus the ratio between their resistances remains unaffected by temperature, keeping the output voltage unaffected by temperature.

Fig. 55. Structure of the strain gauges

Figure. 55 shows the structure of the strain gauges used for this project. They have been designed have 4 strain gauges in 1, internally connected to form a temperature compensated Wheatstone bridge.

Since the differential voltage is in the order of micro to millivolts, the IC used should contain a low noise amplifier (LNA) along with a high-resolution ADC to digitize the strain. 3 ICs have been considered as shown in TABLE III.

All the ICs shown above have a 24-bit Delta-Sigma ADC, so in terms of resolution, they are identical.

The HX711 was used for the first prototype board since it is very commonly used to with load cells and strain gauges. However, despite it having 2 channels, the two channels cannot be configured to have the same amplifier gain, rendering one of the channels useless. The ADS1234 is an attractive option for its quad-channels, which can save board space. However, its high price of HKD 65 is not justifiable as that means a cost per channel of HKD 16.25, around 10 times that of the other two options. The HX710C, despite only having one channel, has an integrated switch to power on and off the strain gauge sensors for reduced power consumption. This can reduce the component count as no external switch is required. At HKD1.2, it is also the most affordable option. Therefore, the HX710C was chosen for the strain gauge amplifier and ADC IC.

Choice of communication protocol (CAN bus)

Since the tube is around 30m long, the strain gauge readings must be transmitted to the ground level while maintaining signal integrity, and at a reasonable speed. It would also be preferable if communication is unaffected by failed tube segments. Two communication protocols have been considered as shown in TABLE IV. CAN bus was chosen due to its robustness and ability to continue functioning with failed tube segments.

Choice of power delivery method and the use of independent LDOs

Proper power delivery is crucial to maintaining proper operation of all tube segments. Since there would be non-negligible voltage drop on the 30m long power cables required to deliver power to all the tube segments, a higher-than-necessary voltage is supplied at the top of the tube, with voltage regulation on each tube to provide proper supply voltages to different parts of the circuit, such as the strain gauge amplifier ICs, the CAN bus transceiver, and the microcontroller. Each PCB requires two supply voltage rails to function properly, 3.3V for the STM32 microcontroller and the strain gauge amplifier ICs, and 5V for the CAN bus transceiver. However, the two supply voltages have different requirements. For the CAN bus transceiver, due to its digital nature, the supply voltage does not have to be particularly clean. However, the strain gauge amplifiers supply power to the strain gauges and perform analog-to-digital conversion. Therefore, it would be preferable for the 3.3V power to be as low-noise as possible. For the sake of efficiency, a buck converter is used to step down the supply voltage to 5V. And for minimizing noise to the analog circuitry, Low Drop-out (LDO) regulators are used to regulate the 5V from the buck converter down to 3.3V for the HX710C and the STM32 microcontroller. Since the PCB is of considerable length (485mm) to reduce the distance between each strain gauge and its corresponding amplifier IC, independent LDOs are placed near the ICs to minimize trace length and voltage drop. The final PCB is shown in Fig. 56 and Fig. 57

4) Software Design:

Acquisition of SG data (CAN bus data format)

As mentioned, CAN bus is used to transmit the readings from the tube segments to the computer, where curve reconstruction takes place. To interface with CAN bus, a commercial USB to CAN bus adaptor is used. The adaptor can receive data from the bus and transmit the received data to the connected computer via a virtual COM port. The data packet transmitted by the tube segments consists of 4 bytes and is of the following format shown in Figure. 58.

3 bytes are required since the HX710C produces 24bit 2s complement integer readings, which can be represented by 24/8 = 3 bytes. For example, if the fifth strain gauge in the tube produced a reading of 0xFFA60E in hexadecimal, the data field would look like Figure.59 in hexadecimal.

Since the CAN bus protocol already contains a CRC field for error detection and correction, no additional error checking is required.

Geometric meaning of curvature

Curvature as a vector with magnitude and direction

The working of the MIT system relies on the fact that the strain experienced by strain gauges attached to the tube is affected by the curvature of the tube. The curvature of a tube at a location is the inverse of the bending radius at that location. Although curvature is generally referred to as a scalar quantity in geometry, there is typically another quantity known as torsion, which describes the direction in which a curve bends in 3D space. When considered together, curvature can be understood as a vector quantity, describing both the magnitude of the bending, and the direction in which bending

TABLE III
ICs CONSIDERATION

	HX711	ADS1234	HX710C
Channels	2	4	1
ADC	24bit Delta-Sigma ADC	24bit Delta-Sigma ADC	24bit Delta-Sigma ADC
Amplifier	PGA with gain 32, 64(only for channel B) or 128 (only available for channel A)	PGA with gain 32, 64 or 128	LNA with fixed gain of 128
Power saving	External BJT for switching power to Wheatstone bridge	None	Integrated switch for switching power to Wheatstone bridge
Price per piece	1.9 HKD	65 HKD	1.2 HKD

TABLE IV
COMMUNICATION PROTOCOLS CONSIDERATION

	HX711	ADS1234	HX710C
Channels	2	4	1
ADC	24bit Delta-Sigma ADC	24bit Delta-Sigma ADC	24bit Delta-Sigma ADC
Amplifier	PGA with gain 32, 64(only for channel B) or 128 (only available for channel A)	PGA with gain 32, 64 or 128	LNA with fixed gain of 128
Power saving	External BJT for switching power to Wheatstone bridge	None	Integrated switch for switching power to Wheatstone bridge
Price per piece	1.9 HKD	65 HKD	1.2 HKD

Fig. 56. Final PCB 1

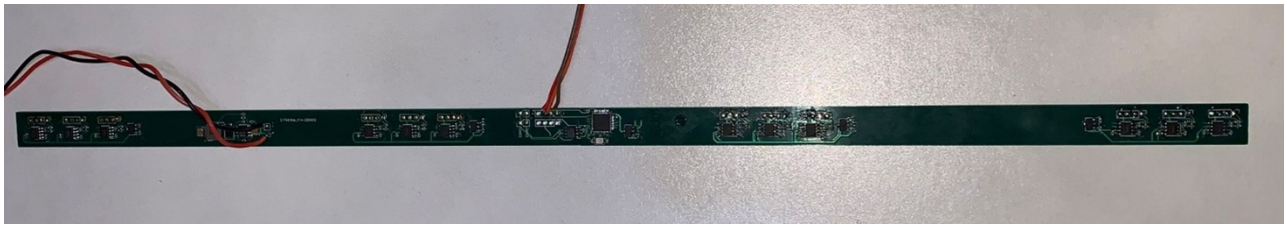

Fig. 57. Final PCB 2

Strain Gauge ID	1st byte of SG reading	2nd byte of SG reading	3rd byte of SG reading

Fig. 58. Data package format

0x05	0xFF	0xA6	0x0E

Fig. 59. Data package format

occurs. With the geometric understanding above in mind, the purpose of the strain gauges becomes clear: to measure the magnitude of the bending and determine in which direction it occurs.

Conversion from strain gauge readings to curvature

Strain gauge readings to strain

As mentioned in the previous section, the relationship between the strain and the output voltage of the Wheatstone bridge:

$$\epsilon = \frac{2 \cdot \frac{V_o}{V_{EX}}}{GF \cdot (1 - \frac{V_o}{V_{EX}})} \tag{7}$$

The readings obtained by from the PCB are 24-bit, 2's complement numbers. To convert from these reading (read) to strain, the following equation is used:

$$\epsilon = \frac{2 \cdot \frac{read}{2^{24}}}{GF \cdot (1 - \frac{read}{2^{24}})} \tag{8}$$

Since the gauging factor of the strain gauges is specified to be 2, the equation becomes:

$$\epsilon = \frac{\frac{read}{2^{24}}}{1 - \frac{read}{2^{24}}} \tag{9}$$

Strain to curvature

The derivation of the strain to curvature equation can be understood using the following geometric explanation.

Consider a strain gauge attached to a tube of length $2R$ and a radius of r. When the tube is straight, both the surface of the tube and the neutral axis of the tube has the same length of $2R$.

Now consider the tube bent into a circle such that the ends meet, with the strain gauge on the outside. The radius formed by the neutral axis now becomes $\frac{2R}{2} = R$. The circumference of the outer surface now becomes $2(R + r)$.

The strain experienced by the strain gauge, neglecting its width, becomes:

$$\epsilon = \Delta L = \frac{2\pi(R + r) - 2\pi R}{2\pi R} = \frac{r}{R} = r\kappa \tag{10}$$

where $\kappa = \frac{1}{R}$, the curvature of the tube.

If the tube bends at an angle θ to the strain gauge, the strain gauge experiences a fraction of the strain as shown below:

$$\epsilon = r\kappa cos(\theta) \tag{11}$$

To solve for both κ and θ, three strain gauges are placed along the circumference of the tube 120° apart to obtain three strains:

$$\epsilon_1 = r\kappa cos(\theta) \tag{12}$$

$$\epsilon_2 = r\kappa cos(\theta - \frac{2\pi}{3}) \tag{13}$$

$$\epsilon_3 = r\kappa cos(\theta - \frac{2\pi}{3}) \tag{14}$$

Resolving the 3 equations above yields the following:

$$\kappa = \frac{C}{3r} \tag{15}$$

$$cos(\theta) = \frac{2\epsilon_1 - \epsilon_2 - \epsilon_3}{C} \tag{16}$$

$$sin(\theta) = \frac{\sqrt{3}(\epsilon_2 - \epsilon_3)}{C} \tag{17}$$

Using these equa tions, the curvature and its direction can be calculated. These equations are also shown to be used in another paper on shape monitoring using strain gauges, in which the exact derivation of the equations was not as shown to much detail. After the curvatures at the triplet locations are obtained, the next step is to interpolate the curvature over the length of the whole tube. As a proof-of-concept, linear interpolation is used for its computational simplicity at this stage. During testing, this already produced excellent results. Other interpolation methods can be investigated as part of future developments of the project to see if better results can be achieved.

Shape reconstruction from curvature data Finite step reconstruction, circle chords, quaternions, linear algebra

The final step is to reconstruct the shape of the tube from the interpolated curvature data. This is done by taking small, straight steps. Within each step, the change in curvature should be extremely small such that it is negligible. In the case of ground movement, the curving radius of the tube is in the order of meters. For the change in curvature to be small over the steps, the steps should be orders of magnitude smaller than the curving radius. Therefore, a reconstruction step of 1mm is chosen.

Reconstruction begins with a vertical reference step. This can either be the top or bottom of the tube. In actual ground movement, starting from the bottom is preferable since the tube is fixed to the bedrock at the bottom, providing a fixed reference point. However, for illustrative purposes, the explanation below will start from the top. The curving radius will also be smaller relative to the reconstruction step for easier illustration.

Reconstruction steps:

Step 1: Start with a vertical straight line with length 1mm as shown in Fig.60

Fig. 60. Reconstruction step 1

Step 2: Construct a circle of radius 1/, where is the curvature at that point, and position it such that the end points of the previously constructed straight line intersect the circle as shown in Fig.61

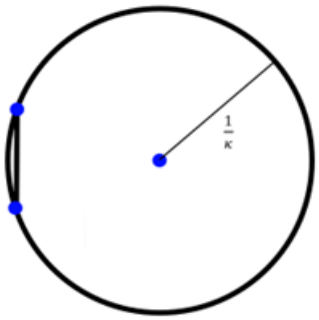

Fig. 61. Reconstruction step 2

Step 3: Construct another 1mm long line such that the one end touches the previous line and the other end intersects the circle as shown in Fig.62

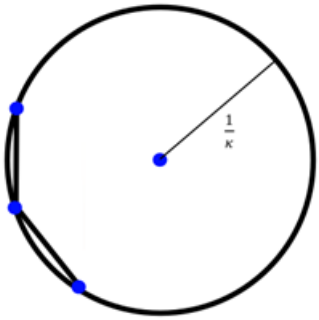

Fig. 62. Reconstruction step 3

Step 4: Repeat the steps 2 and 3 with the interpolated curvature at each location as shown in Fig.63

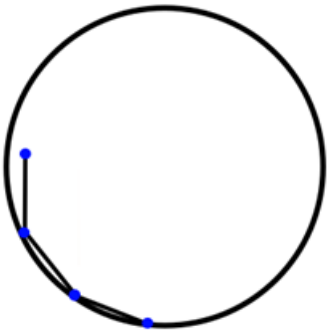

Fig. 63. Reconstruction step 4

By iteratively performing the steps above until the reconstruction reaches the end, the entire shape of the tube can be reconstructed. The steps shown above are illustrated in 2D, but it can also be applied to shape reconstruction in 3D. The only difference is that the circles can now be constructed in any orientation, and that the twisting of the lines in 3D space must be taken into account to avoid false reconstruction. In step 2 of the reconstruction, a line is constructed with the circle. In the actual implementation of the software, the angle Φ between the two lines is calculated using the circle using the following formula:

$$\Phi = \pi - 2cos^{-1}(step \cdot \frac{\kappa}{2}) \tag{18}$$

Where step is the step size in mm, and κ the curvature in mm^{-1} To perform step 3 in software, the previous line segment is assumed to be vertical, and another vertical straight line is rotated to the desired orientation relative to the previous segment in 3D space using quaternions. A rotation quaternion is constructed using θ and Φ

$$quant_{rot} = cos(\frac{\Phi}{2}) + sin(\theta) \cdot sin(\frac{\Phi}{2})i + cos(\theta) \cdot sin(\frac{\Phi}{2})j \tag{19}$$

Afterwards, the vertical straight line (which is the k vector in linear algebra), is rotated using the quaternion by the quaternion multiplication.

$$k_{rot} = quat_{rot} \cdot k \cdot quant^*_{rot} \tag{20}$$

$quat^*_{rot}$ denotes conjugate of the quaternion $quat_{rot}$

In the same manner, the i and j vectors are rotated as well. This is to capture any rotation in the tube, which cannot be captured by the k vector alone (It is important to note that even though the tube itself is assumed to have no twisting, the k vector can still be rotated about itself due to bending in more than one direction. It is crucial that this rotation is captured, as it alters the alignment of the strain gauges) Finally, since the previous line segment may not be vertical, i_{rot}, j_{rot}, and k_{rot} must be rotated with respect to the previous line segment. This is done by one matrix multiplication

$$\begin{bmatrix} i_{step} \\ j_{step} \\ k_{step} \end{bmatrix} = \begin{bmatrix} i_{prev} & j_{prev} & k_{prev} \end{bmatrix} \begin{bmatrix} i_{rot} \\ j_{rot} \\ k_{rot} \end{bmatrix} \tag{21}$$

The resultant vector can be added to the previous end point of the reconstruction to give the coordinates of the next point. Finally, the assignment below is done to update the vectors:

$$\begin{bmatrix} i_{prev} \\ j_{prev} \\ k_{prev} \end{bmatrix} = \begin{bmatrix} i_{step} \\ j_{step} \\ k_{step} \end{bmatrix} \tag{22}$$

The steps above can now be performed iteratively to reconstruct the entire length of the tube.

Optimization of SG spacing by comparison with dial indicated readings

Theoretically, if the curvature of the tube at every location is known, the shape of the tube can be reconstructed perfectly. In practice, however, it is impossible to measure the curvature at every location, as it would take an infinite number of strain gauges that are each infinitely small. A practical, manufacturable design should instead have strain gauges attached to

the tube at regular intervals to sample the curvature at various points, which allows the curvature at other locations to be estimated by interpolation of the sampled readings. Deciding the spacing of the strain gauges, however, is a delicate trade-off between accuracy and cost. If the strain gauges are placed too far apart, there would not be enough samples of the curvature to produce an accurate reconstruction of the tube. On the other hand, reducing the spacing would increase the accuracy, but would also increase the number of strain gauges required and therefore the total cost of the system. Optimization of the spacing therefore refers to finding the largest spacing that would still yield results that are sufficiently accurate.

To determine the optimal spacing, a PVC pipe was prepared with strain gauges stuck at 50mm intervals. This would allow us to test any spacing that is a multiple of 50mm, including 100mm, 150mm, 200mm and so on. The exact shape of the tube is then probed using a dial indicator. After then reconstructing the shape using the strain gauge readings at various spacings, the reconstructed curves and the probed curve are overlaid and compared as shown in Fig. 67.

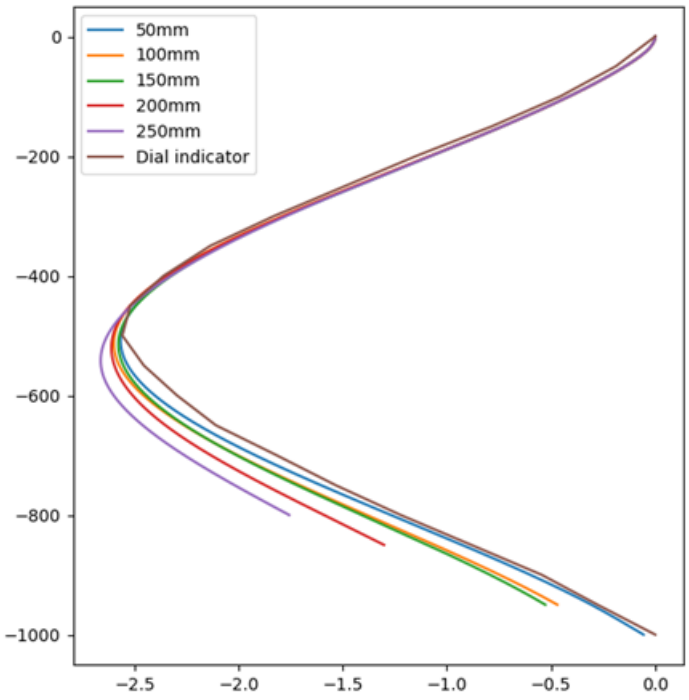

Fig. 64. Reconstructed curves

From the above results, it is clear that error increases with sensor spacing. It is concluded that 150mm provides sufficiently accurate results while keeping the number of strain gauge sensors required to a minimum.

C. Testing setup

The test setup uses the final version of the test rig mentioned in the mechanical design section where the test rig with 8 pushers is mounted vertically upright. The tube is pushed in 4 directions and be bent in a ”C” or ”S” shape.

D. Testing Result

With our latest prototype, we are able to bend the tube and show its deformation digitally.

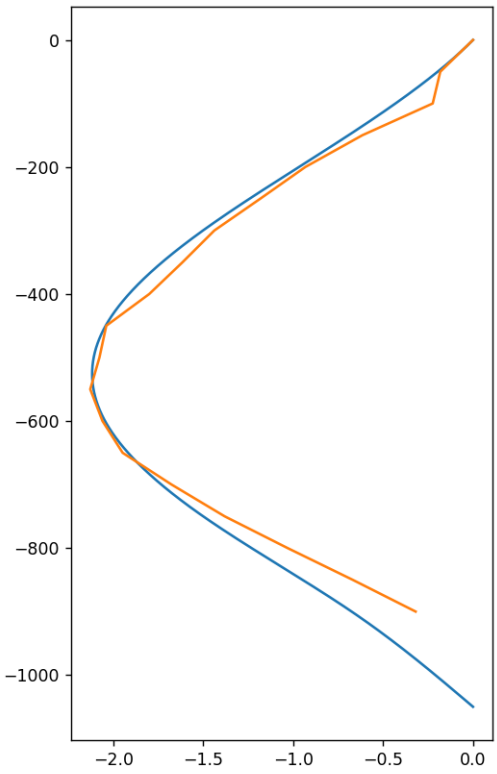

Fig. 65. Reconstruction against probed readings

As shown in Figure 65, the reconstructed curve matches the actual shape of the tube obtained by dial indication closely, The maximum deflection is spot on and the maximum error is 0.25mm.

Figure 66 shows the tube being bent into a C-shape towards the Y-axis. Figure 67 shows the reconstructed shape when bent into this position. The shape is accurately reconstructed and the maximum deflection is measured to be at 90 . This shows that apart from the shape, the strain gauge triplets are able to accurately detect the direction of curvature.

E. Potential Improvement

During testing, we found out that the readings are not as accurate as of the current market solutions. One reason for this error could be derived from not aligning the sensors accurately. Currently, the sensors are aligned by hand and through visual inspection. Errors would be induced when manually sticking many sensors. Therefore, the sensor alignment could be improved a lot by using pick and place machines to align and stick the strain gauges.

Fig. 66. Tube bent into the Y-axis

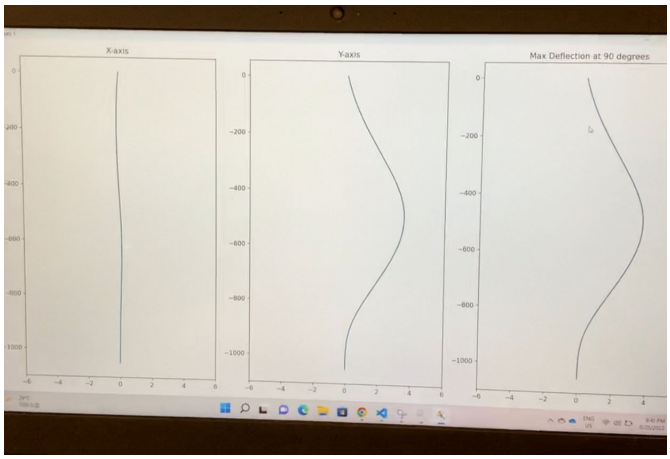

Fig. 67. Reconstruction of the bent tube shown above

VIII. Summary and Conclusion

This document explained two solutions targeting intelligent real-time land-movement monitoring in details. The team start from defining the problem by interview and desk research. The topic of land-movement monitoring is chosen, and the team focus on making land-movement monitoring process real-time and user friendly. After generating the idea, functioning prototypes are built and tests and experiments are made. Though there can be improvement, this document argues that the proposed solution met the expectation of the team. Both method gives good testing result and answer to the problem statement. The team hope that this method can be implemented in field and improved in the future and better monitoring can be done to make construction safer and more convenient.

References

[1] "inclinometer(clinometer),"A Dictionary of Mechanical Engineering (ed.2), Oxford University Press, 2019
[2] D. S. Timothy, "Slope inclinometers for landslides," in Landslides, August 2008
[3] Geomotion Australia "soil instruments digital inclinometer pro" YouTube, 2017. Available: https://www.youtube.com/watch?v=KTKWmJ9rODw
[4] Measurand Videos "Simple and Easy: ShapeArray Installation" YouTube, 2019. Available: https://www.youtube.com/watch?v=VG7diET86G4&t=74s
[5] serial library. Available: https://github.com/wjwwood/serial
[6] JSON IO library. Available: https://github.com/Nomango/configor